Journal of Catalysis 283 (2011) 161–167

Contents lists available at SciVerse ScienceDirect

Journal of Catalysis

journal homepage: www.elsevier.com/locate/jcat

Low-temperature aerobic oxidation of decane using an oxygen-free radical initiator

Rhys Lloyd [a], Robert L. Jenkins [a], Marco Piccinini [a], Qian He [b], Christopher J. Kiely [b], Albert F. Carley [a], Stanislaw E. Golunski [a], Donald Bethell [a], Jonathan K. Bartley [a], Graham J. Hutchings [a,*]

[a] Cardiff Catalysis Institute, School of Chemistry, Cardiff University, Park Place, Cardiff CF10 3AT, UK
[b] Department of Materials Science and Engineering, Lehigh University, Bethlehem, PA 18015-3195, USA

ARTICLE INFO

Article history:
Received 26 January 2011
Revised 26 June 2011
Accepted 3 August 2011
Available online 15 September 2011

Keywords:
Alkane oxidation
Radical initiator
Cerium oxide
Gold catalysis

ABSTRACT

The direct selective oxidation of long chain alkanes by O_2 is a highly demanding reaction. We have shown that it is possible to oxidise *n*-decane in the presence of the oxygen-free radical initiator azobisisobutyronitrile. Formation of a range of oxygenated products has been observed under relatively mild conditions (70 °C in air). Although the presence of a catalyst is not essential when the initiator is used, ceria-based catalysts have been found to increase the selectivity to alcohols by modifying the oxyfunctionalisation of decane.

1. Introduction

Catalytic selective oxidations account for a significant proportion of modern commercial chemical processes [1]. One of the most important applications of selective oxidation is the functionalisation of hydrocarbons. With industry moving towards the lower-environmental-impact and lower-cost processes, the direct oxidation of alkanes has become a key priority [1,2]. Current commercial selective alkane oxidation processes include the production of cyclohexanone and cyclohexanol from cyclohexane (KA oil, 10^6 tons/year) [2], the feedstock chemicals for nylon and maleic anhydride primarily from butane (10^6 tons/year) [3]. Another notable hydrocarbon oxidation is the production of terephthalic acid from *p*-xylene (3×10^6 tons/year), used in the synthesis of poly(ethylene terephthalate) [2].

Direct alkane autoxidation, which avoids an initial dehydrogenation step, proceeds by a free-radical chain mechanism producing hydroperoxides [4], which may undergo consecutive complex reactions forming ketones, alcohols and carboxylic acids [5]. Potential sources for the reaction initiation include the thermal generation of radicals or from impurities or initiators [4,6]. Various radical initiators have been used for the oxidation of alkanes. Twigg [7] used benzoyl peroxide to initiate the oxidation of decane. Propagation occurs predominantly by the addition of oxygen to alkyl radicals to give alkylperoxy radicals that further react with alkane molecules, producing hydroperoxides and alkyl radicals. Once initiation has occurred, the reaction of alkylperoxy radicals with alkane molecules is rate limiting at low temperatures, whereas the addition of oxygen to alkyl radicals is rate limiting at high temperatures and low oxygen concentrations. Consequently, the change in alkylperoxy and alkyl concentrations will affect consecutive reactions and hence the product distribution [5]. Termination may occur by the combination of radical species or the formation of relatively stable species (reaction with a radical stabiliser). The hydroperoxides formed may undergo thermal or catalytic decomposition by free-radical or ionic mechanisms. Decomposition of the hydroperoxides produced may therefore both promote the reaction and direct the product distribution.

Gold catalysts are often used to decompose the radical initiators to enhance the rate of reaction [8]. Numerous reports on the catalytic decomposition of radical initiators over gold surfaces have been published, including hydrogen peroxide [9] and organic peroxides such as cumene hydroperoxide (CHP) [10]. Recently, the oxygen-free radical initiator azobisisobutyronitrile (AIBN) has been reported to enhance significantly both the conversion and selectivity for the aerobic epoxidation of cyclohexene and 1-octene over gold nanoparticles supported on nano-ceria or MCM-41 supports [11,12]. Other radical initiators (benzoyl peroxide, tert-butyl peroxybenzoate, tert-butyl hydroperoxide, cumene hydroperoxide and 2,2′-azobis(2-methylpropionamidine)dihydrochloride) were tested with gold on MCM-41, but they were all found to give lower conversions and selectivities than AIBN. The addition of 2,2,6,6-tetramethylpiperidin-1-yloxy (TEMPO, which reacts with other radicals thus shortening their lifetimes) was found to reduce the conversion dramatically when added together with AIBN and the gold catalyst. If TEMPO was added at the

* Corresponding author. Fax: +44 (0)29 208 74030.
E-mail address: hutch@cf.ac.uk (G.J. Hutchings).

0021-9517/$ - see front matter © 2011 Elsevier Inc. All rights reserved.
doi:10.1016/j.jcat.2011.08.003

beginning of the reaction, the selectivity to the epoxide was also found to be lower, but if it was added after the start of the reaction, only the conversion was observed to decrease. Corma and co-workers [11–13] proposed the reaction to proceed by AIBN reacting with gold particles to form an alkylgold intermediate that can catalytically produce hydroperoxides. However, the increase in selectivity seen with AIBN compared to other radical initiators indicates a mechanism, such as a direct O-transfer, that by-passes the usual radical process with hydroperoxides. The results obtained upon addition of TEMPO suggest that when it is added at the beginning of the reaction, it inhibits the selective mechanism. Since, if TEMPO is added later, it does not affect the reaction mechanism, the mechanism(s) must still depend on the generation of radical species.

The radical initiator AIBN has been used for the oxidation of heptane at 100 °C; however, using small amounts of initiator, it was reported that the molar amounts of ketones and alcohols formed were significantly less than the amount of initiator used [14]. The inefficiency of AIBN was attributed to the dimerisation of radicals formed [15–18] and the formation of 2-cyanopropan-2-ylperoxy radicals, which act as radical trap [14].

Gold catalysts have previously been used to selectively oxidise cyclohexane [19–25] and *n*-hexadecane [26] and have been shown to be active when supported on silica [19–21], graphite [22], alumina [23] or ZSM-5 [24]. For the oxidation of cyclohexane, the selectivity towards alcohols and ketones has been shown to shift with conversion, alcohols being favoured at low conversions [22]. The results of a recent study suggest that the reaction proceeds by essentially the same mechanism as in autoxidation, with the gold playing a role in directing the specific pathway [27]. Many of these previous studies have been carried out with the more reactive cyclic alkanes, in which all carbon atoms in the molecules are equivalent. In this study, we have investigated decane as a model linear alkane that adds a degree of complexity to the regioselectivity of the reaction over the cyclic systems.

Long chain linear alkanes are relatively inexpensive feedstocks available from the Fischer Tropsch process [28]. The selective oxidation of alkanes, especially to linear primary alcohols, is of industrial importance for the production of plasticizers and surfactants for detergents [29]. It is, however, considerably more difficult to selectively oxidise long chain alkanes, such as decane, than shorter chain cyclic alkanes (often used as model reactants) or alkenes of the equivalent length because of their tendency to dehydrogenate and form coke deposits as well as greater regioselectivity demands [30].

The aim of this work is to investigate the effect of radical initiators on the aerobic oxidation of *n*-decane. In particular, the combination of the radical initiator AIBN with gold supported on nano-ceria has been studied for alkane oxidation. It is proposed, based on the previous work of Corma and co-workers [11–13], that the generation of a sterically hindered hydroperoxide may lead to terminal selectivity in the H-abstraction from the alkane. The best reported terminal selectivity for linear alkane oxidation in the literature has been reported by Zhan et al. for *n*-hexane oxidation with Mn-exchanged zeolites [31]. This gave 24% terminal selectivity at 0.007% conversion, which drops to 10% terminal selectivity at 0.1% conversion. This study was undertaken at low temperature ($\leqslant$90 °C) to limit conversion and determine whether high terminal selectivity could be achieved using this methodology.

2. Experimental

Au was dispersed onto nanoCeO$_2$ (VP AdNano® Ceria 90, Degussa AG) by deposition precipitation, using a previously reported method [12]. An aqueous solution containing HAuCl$_4$ (0.140 g in 5.7 ml H$_2$O) was adjusted to pH 10 by the addition of NaOH (0.2 M). This solution was added to a slurry comprising nanoCeO$_2$ (1.260 g in 25 ml H$_2$O), and the pH was again adjusted to 10 by the addition of NaOH (0.2 M). The resulting mixture was stirred vigorously for 18 h after which the solid was isolated by filtration and washed thoroughly to remove chloride ions and dried (110 °C, 16 h). The catalyst (Au/nanoCeO$_2$) was not calcined.

Samples for examination by scanning transmission electron microscopy (STEM) were prepared by dispersing the dry catalyst powder onto a holey carbon film supported by a 300 mesh copper TEM grid. STEM high-angle annular dark-field (HAADF) images and STEM bright field images (BF) of the catalysts were obtained using an aberration corrected JEOL 2200FS (S)TEM operating at 200 kV.

X-ray photoelectron spectra were recorded on a Kratos Axis Ultra DLD spectrometer using a monochromatised AlKα X-ray source (120 W). Spectra were recorded at analyser pass energies of either 160 eV (survey scans) or 40 eV (detailed scans). Binding energies are referenced to the C(1s) binding energy of adventitious carbon contamination, which is taken to be 284.7 eV.

The BET surface area of the prepared Au/nanoCeO$_2$ was measured by N$_2$ adsorption at −196 °C using a Micromeritics Gemini 2360 surface area analyser. A Varian 55B AA spectrometer was used to determine the Au content of the material.

For comparison in addition to the prepared Au/nanoCeO$_2$ and nano-CeO$_2$ support used, the catalytic properties of a standard ceria powder (Aldrich), a high surface area titania (Degussa, P25) and ZSM-5 (Zeolyst, SiO$_2$:Al$_2$O$_3$ = 30, calcined at 550 °C in static air for 4 h) were tested.

Reactions were performed at 70 °C under reflux at atmospheric pressure in air, or at 90 °C and 1.2 MPa O$_2$, both with and without a radical initiator. The tests at atmospheric pressure were performed with decane (10 g) and AIBN (50 mg) in 25 ml glass round-bottom flasks under reflux (70 °C, 20 h) with stirring. High-pressure reactions were performed under conditions similar to those used by Corma and co-workers [12]. Decane (7.68 g, 54 mmol) or 1-octene (6.06 g, 54 mmol), catalyst (100 mg) and AIBN or CHP (30 mg) were placed in 12 ml stainless-steel autoclave reactors. The autoclaves were flushed twice with O$_2$ and pressurised with 1.2 MPa O$_2$, then heated to 90 °C for 2 h or 20 h with stirring. Reactions were quenched using an ice bath.

Reaction products were quantified using a Varian 3380 GC fitted with a CP-Wax 52CB column, and FID and GC injections were duplicated and the average reported. For the decane reactions, 1,2,4-trichlorobenzene (150 μl) was used as an internal standard. Hydroperoxide concentrations of selected reactions were measured by the reduction method with triphenylphosphine (PPh$_3$) [32,33]. To an aliquot of the reaction products, 10% PPh$_3$ in acetone was added (to give an approximate weight ratio of 3:1) and left to equilibrate for at least 20 min prior to the GC analysis. The hydroperoxide species are selectively reduced to alcohols upon addition of PPh$_3$, as shown in Eq. (1). Assuming in the absence of PPh$_3$, the hydroperoxides decompose into ketones and alcohols upon GC analysis in equal proportions then the hydroperoxide concentrations can be estimated.

$$\mathrm{ROOH} + \mathrm{PPh_3} \rightarrow \mathrm{ROH} + \mathrm{POPh_3} \quad (1)$$

Decane conversion was calculated from the molar concentrations using the following equation:

$$\text{Conversion} = \left[\sum \text{mol productions} \times \text{Cn}\right] \Big/ \left(\left[\sum \text{mol reactant remaining} \times \text{Cn}\right] + \left[\sum \text{mol products} \times \text{Cn}\right]\right) \times 100\%$$

where Cn = carbon number (i.e. 10 for decane).

Carbon balance (C bal) was calculated also using molar concentrations using the following equation:

$$\text{C bal} = \left[\sum \text{mol reactant remaining} \times \text{Cn}\right] + \left[\sum \text{mol products} \times \text{Cn}\right] / \left[\sum \text{mol reactant} \times \text{Cn}\right] \times 100\%$$

where the reactant remaining and product concentrations are calculated from the gas chromatographic data and the reactant concentration is based on the weight of the sample. Errors in this analysis can be introduced due to losses incurred during the transfer of solutions and the inaccuracy in using assumed relative response factors for diones as well as the carbon number for unidentified products. Response factors for all reported alcohols, ketones and acids were experimentally determined. GCMS was also performed, to confirm product identification, using an Agilent 6890 GC also fitted with a CP-Wax 52CB column and a Waters GCT Premier orthogonal acceleration time-of-flight mass spectrometer.

3. Results and discussion

In Table 1, the BET surface area, pore volume and gold content of the prepared Au/nanoCeO$_2$ catalyst are shown. No significant change in surface area is observed upon loading gold onto the nanoCeO$_2$ support, but the pore volume decreased slightly. The Au/nanoCeO$_2$ catalyst was found to have a higher gold content than previously reported materials prepared using this method on higher surface area ceria supports [12], which suggests that the ceria support used here has a stronger affinity for the deposition precipitation of the gold complex from solution. The Au/nanoCeO$_2$ 'dried-only' catalyst was studied by aberration corrected scanning transmission electron microscopy in order to elucidate how the Au was dispersed on the nano-ceria support surface. A representative lower magnification BF- and HAADF–STEM image pair is shown in Fig. 1. The support material has a particle size range of about 5–20 nm, and the BF-STEM image showed phase contrast fringes characteristic of the CeO$_2$ lattice. The Au species can only barely be discerned by mass-thickness contrast as small dark flecks in the BF-STEM image. However, in the corresponding HAADF–STEM image, the Au clusters can be readily distinguished as bright features by virtue of their higher Z-contrast (Z_{Au} = 79, Z_{Ce} = 58). The Au clusters were quite monodispersed, being 1–2 nm sized, as shown in the corresponding particle size histogram. A higher magnification HAADF–STEM image of the same sample is shown in Fig. 2, in which some of the Au species are imaged in profile. They clearly have a thickness of 2–3 atomic layers, suggesting that the 1–2-nm Au nano-clusters are more three dimensional in nature as opposed to monolayer rafts.

Table 1
Surface area and Au loading.

Material	[Au] (wt.%)	BET surface area (m^2/g)	Pore volume (ml/g)
NanoCeO$_2$	–	77	0.59
Au/nanoCeO$_2$	4.3	78	0.33

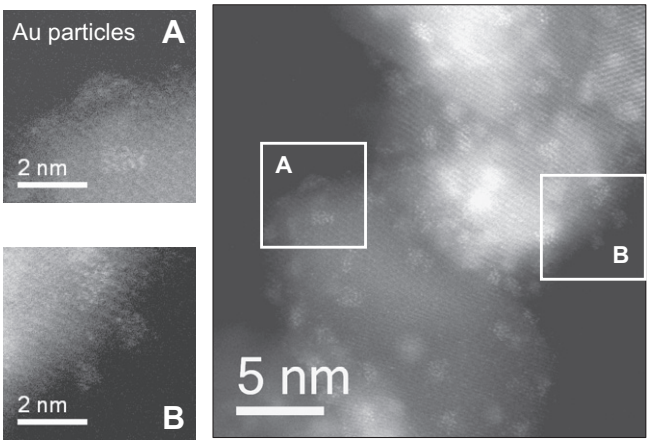

Fig. 2. Representative higher magnification STEM–HAADF images of the Au/nanoCeO$_2$ 'dried-only' catalyst. Expanded views of the regions delineated as A and B show some of the supported Au species in profile view. It is clear that they have a thickness of two to three atomic layers and are more 'particle-like' than 'raft-like' in morphology.

XPS analysis of the Au/nanoCeO$_2$ catalyst was carried out to determine the oxidation state of the gold. The initial Au(4f) acquisition (Fig. 3a) shows that the gold in the catalyst was predominantly in the 3+ oxidation state, but these species reduced significantly to Au^o after continued exposure to X-rays (Fig. 3b). The initial state of the surface (at t = 0 irradiation time) is likely to be almost entirely Au^{3+}.

No conversion was detected for the blank decane reaction, at 70 °C, under reflux at atmospheric pressure in air for 20 h or at 90 °C and 1.2 MPa O$_2$ for 2 h, without a radical initiator or catalyst. Oxidation of decane with AIBN under these conditions was found to produce a range of oxygenated products. AIBN starts to decompose to form radicals at above 60 °C (Fig. 4), although the rate of decomposition is slow at these low temperatures and the half-life is in the order of tens of hours [34]. A summary of the products formed is given in Table 2, with a more comprehensive breakdown given in Table 3. The raw data in Table 3 has been recalculated based on the data obtained with and without PPh$_3$ addition to determine the amount of peroxide species (see the experimental section for details), which is shown in the summary in Table 2. Decane conversion using AIBN is found to increase at higher temperature and pressure, although the selectivity to peroxide species is found to decrease (Table 2). The radical initiator is proposed to produce peroxide species which then form alcohols and carbonyl compounds by consecutive reactions [4]. At higher temperature and pressure, it is considered that more peroxides are produced, hence the higher conversion. However, because at higher temperatures, the product-determining steps are faster, the selectivity to peroxides is lower.

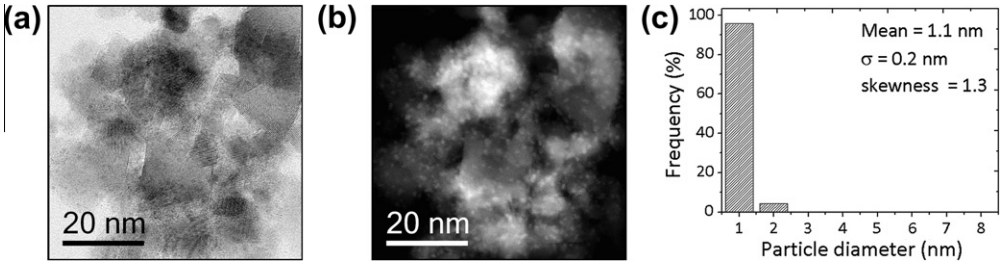

Fig. 1. Representative lower magnification BF (a) and HAADF (b) STEM image pair of the Au/nanoCeO$_2$ 'dried-only' catalyst and the corresponding gold particle size distribution (c).

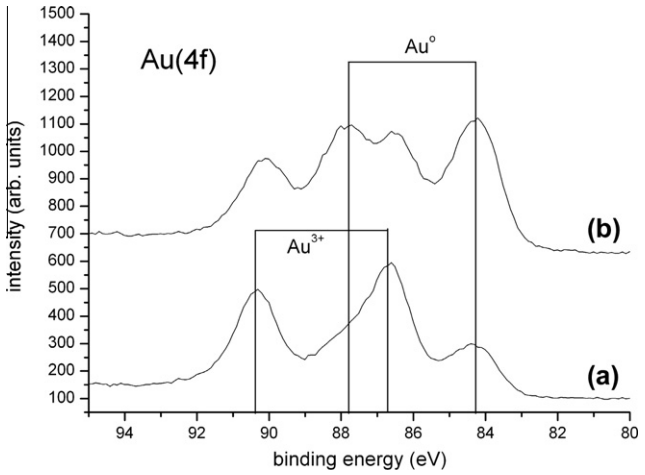

Fig. 3. Au(4f) spectra for the dried Au/nanoCeO$_2$ catalyst showing the sensitivity of the Au oxidation state to X-irradiation: (a) initial measurement, accumulated irradiation time = 600 s; (b) repeated measurement, accumulated irradiation time = 3160 s.

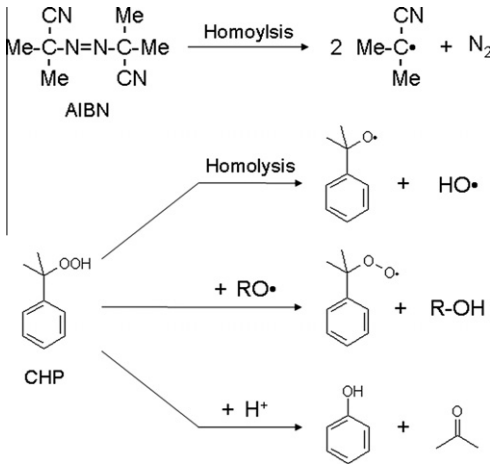

Fig. 4. Decomposition pathways of AIBN and CHP.

Short-chain carboxylic acids are formed in addition to decanoic acid. CO*x* was not observed under the reaction conditions employed, which indicates that the mechanism for the formation of the short-chain acids is not the same as the one proposed by Hermans et al. for cyclohexane conversion [2]. For cyclohexane, ring opening gives ω-formyl radicals (·CH$_2$(CH$_2$)$_4$CHO) that allow further oxyfunctionalisation at the ω position. CO_2 is eliminated from acyloxy radicals (·OOC (CH$_2$)$_4$COOH) that subsequently form to give a C_5 ω-formyl radical.

For linear alkanes, short-chain acids are thought to form due to breaking of C–C bonds adjacent to an alkoxy radical (CH$_3$(CH$_2$)$_n$(CHO·)(CH$_2$)$_m$CH$_3$) formed by the oxidation of a secondary carbon. The bond breaking is analogous to the cyclohexane mechanism, but the linear alkane will form two new species, an oxygenated fragment (CH$_3$(CH$_2$)$_n$CHO) and an alkyl radical (·CH$_2$(CH$_2$)$_m$CH$_3$) that can both be oxidised to carboxylic acids. This process was studied widely in Germany in the 1940s and Eastern Europe in the 1960s and 1970s to produce fat and has been used industrially in the past to oxidise *n*-butane to two molecules of acetic acid with cobalt catalysts [35].

Identification of the products by GCMS revealed that the oxidation of decane at 70 °C produced phthalic anhydride, cyclodecane, hexenone and branched alkenes in addition to the products reported in Tables 2 and 3. AIBN and dimethyl-N-(2-cyano-2-propyl)-ketenimine (the dimer formed from the radicals generated from AIBN) were also detected by GCMS, but no other AIBN decomposition products were found.

At a longer reaction time (20 h, 90 °C, 1.2 MPa O_2), a low blank decane conversion is observed (Table 4). Oxidation of decane with AIBN under these conditions results in a conversion that is significantly higher than the theoretical stoichiometric conversion from the two radicals generated from each AIBN molecule alone (0.68%). Given the observed conversion and that radicals generated from AIBN have been reported to readily form dimers [15–18], it is proposed that only a limited proportion of radicals created from AIBN form oxidation chain reactions.

The Au/nanoCeO$_2$ catalyst was found to be inactive for the oxidation of decane at 90 °C and 1.2 MPa O_2, over 2 h, without a radical initiator. Upon addition of both the Au/nanoCeO$_2$ catalyst and AIBN to decane, at 90 °C and 1.2 MPa O_2, over 2 h and 20 h, there is a small decrease in conversion, and the selectivity to C_{10} alcohols and peroxides increases very slightly compared with the reaction of AIBN and decane (Tables 2 and 3). Addition of the nanoCeO$_2$ support with AIBN to decane, at 90 °C and 1.2 MPa O_2, over 2 h or 20 h was found to decrease the conversion even more than Au/nanoCeO$_2$ and AIBN, under the same conditions, and increase the ratio of alcohols to ketones (Tables 2 and 3). The nanoCeO$_2$ support was found to be inactive for the oxidation of decane at 90 °C and 1.2 MPa O_2, over 2 h, without a radical initiator, but over 20 h a low conversion was detected (Table 4).

Results for the oxidation of decane over either a standard CeO$_2$ powder, TiO$_2$ or ZSM-5 with AIBN, at 90 °C and 1.2 MPa O_2 for 20 h are shown in Table 4. The standard CeO$_2$ powder and AIBN was found to give the same conversion as using AIBN alone but the

Table 2
Oxidation of *n*-decane using AIBN, with and without catalyst.

Initiator/catalyst	Conditions	Conversion%	Selectivity%						
			C_{10} ketones	C_{10} internal alcohols	C_{10} internal peroxides[c]	C_{10} terminal[d]	C_{10} diones	C_1–C_9 acids	Others
AIBN[a]	70 °C, 20 h, air, reflux	0.26	16.4	0.5	29.7	0.6	8.4	3.1	41.3
AIBN[b]	90 °C, 2 h, 1.2 MPa O_2	0.49	35.2	4.1	15.4	0.1	11.7	3.9	29.6
AIBN + Au/nanoCeO$_2$[b]	90 °C, 2 h, 1.2 MPa O_2	0.46	19.8	6.9	19.4	0.1	10.7	4.3	38.8
AIBN + nanoCeO$_2$[b]	90 °C, 2 h, 1.2 MPa O_2	0.36	26.6	12.0	25.4	1.4	9.6	3.2	21.8
AIBN[b]	90 °C, 20 h, 1.2 MPa O_2	1.13	58.1	0.9	12.6	2.1	7.0	12.3	6.9
AIBN + Au/nanoCeO$_2$[b]	90 °C, 20 h, 1.2 MPa O_2	0.87	25.2	19.3	11.7	1.6	11.4	21.4	9.5
AIBN + nanoCeO$_2$[b]	90 °C, 20 h, 1.2 MPa O_2	0.78	15.6	23.7	10.2	1.5	11.0	21.9	16.2

[a] 10.0 g decane, 50 mg AIBN.
[b] 7.69 g decane, 30 mg AIBN.
[c] Secondary decyl hydroperoxides.
[d] C_{10} terminal includes 1-decanol, 1-decyl hydroperoxide and decanoic acid.

Table 3
Product breakdown for the oxidation of *n*-decane, with and without AIBN, with and without catalyst, and with and without addition of PPh_3 (for selected reactions).

Catalyst/initiator	Conditions		Conv.%	Selectivity/%[c]																C bal.%
				C_{10} 5/4-one	C_{10} 3-one	C_{10} 2-one	C_{10} 4-ol	C_{10} 3-ol	C_{10} 2-ol	C_{10} 1-ol	C_{10} acid	C_9 acid	C_8 acid	C_7 acid	C_5 acid	C_4 acid	C_3 acid	C_2 acid	C_{10} diones	Others	
AIBN[a]	70 °C, 20 h, air, reflux	–	0.26	15.0	7.4	9.2	6.8	3.6	4.9	0.3	0	0.4	0.1	1.2	1.2	0	0	0.3	8.4	41.2	93
		+PPh_3	0.27	11.7	5.8	6.1	18.7	10.0	14.6	0.9	0	0.9	0.3	1.6	0	0	0	0	6.6	23.0	86
AIBN[b]	90 °C, 2 h, 1.2 MPa O_2	–	0.49	20.1	10.0	12.7	4.6	2.7	4.6	0.1	0	0.3	0	1.3	1.4	0.3	0	0.6	11.7	29.6	83
		+PPh_3	0.45	19.6	9.6	11.8	9.3	5.3	8.4	0	0	0.5	0	1.9	0.4	0	0	0.2	11.2	21.7	77
Au/nanoCeO_x + AIBN[b]	90 °C, 2 h, 1.2 MPa O_2	–	0.45	14.0	6.6	8.8	6.6	3.8	6.3	0	0	0.7	0	0.8	1.3	0.3	0	1.2	10.7	38.9	94
		+PPh_3	0.47	11.2	5.9	7.4	13.6	7.8	11.3	0	0.1	0.9	0.1	2.8	0.3	0.1	0.2	0.7	12.2	25.4	81
$NanoCeO_2$ + AIBN[b]	90 °C, 2 h, 1.2 MPa O_2	–	0.36	17.4	8.9	13.1	11.4	5.5	7.8	0.9	0.4	0	0	1.6	1.1	0.5	0	0	9.6	21.8	105
		+PPh_3	0.40	14.0	6.4	10.2	18.7	10.0	14.3	1.1	1.4	0	0	0.7	0	0	0	0	4.0	19.1	114
Blank[b]	90 °C, 20 h, 1.2 MPa O_2	–	0.028	21.9	12.2	21.2	6.0	2.6	4.6	0	0	0	0	0	0	0	0	0	0	31.5	95
AIBN[b]	90 °C, 20 h, 1.2 MPa O_2	–	1.13	27.2	17.9	19.3	3.0	1.7	2.8	1.1	0.8	0	0.3	2.0	3.7	3.5	2.8	0	7.0	6.9	89
		+PPh_3	1.47	23.7	15.1	16.3	5.4	3.1	4.9	0.7	1.0	0	0.3	1.0	2.4	2.1	3.2	0	8.7	12.1	99
Au/nanoCeO_2 + AIBN[b]	90 °C, 20 h, 1.2 MPa O_2	–	0.87	12.5	7.8	10.9	10.3	6.1	8.8	0.9	0.5	0.2	0.6	1.3	5.3	6.4	3.4	4.3	11.4	9.5	79
		+PPh_3	0.88	11.6	8.1	9.7	16.0	8.7	11.5	1.3	0.8	0.3	0.3	1.4	4.1	3.6	3.8	0.5	10.7	7.6	89
$NanoCeO_2$[b]	90 °C, 20 h, 1.2 MPa O_2	–	0.11	11.1	5.5	11.1	8.7	4.1	4.9	2.7	1.7	1.0	0	0.9	5.9	8.1	8.7	0	11.3	14.3	107
$NanoCeO_2$ + AIBN[b]	90 °C, 20 h, 1.2 MPa O_2	–	0.78	5.3	8.0	11.0	10.3	5.9	9.1	1.0	0.4	0.4	0.4	1.0	4.2	4.6	4.3	7.1	11.0	16.0	70
		+PPh_3	0.79	11.2	7.8	9.3	13.2	7.3	10.2	1.0	0.5	0.3	0.2	2.2	3.0	3.1	2.5	3.2	10.3	14.6	78
Aldrich CeO_2 + AIBN[b]	90 °C, 20 h, 1.2 MPa O_2	–	1.13	20.0	10.2	15.3	7.4	4.1	5.9	0.8	0.9	0.1	0.4	3.2	5.2	3.9	2.5	0	10.6	9.5	107
TiO_2 + AIBN[b]	90 °C, 20 h, 1.2 MPa O_2	–	0.58	15.3	7.6	11.7	12.8	7.0	10.0	1.1	0.8	0	0.2	1.5	1.4	2.3	0	0	10.3	18.0	107
ZSM-5 + AIBN[b]	90 °C, 20 h, 1.2 MPa O_2	–	0.91	25.6	13.2	18.0	5.3	2.9	4.3	0.5	1.9	0	0.5	2.2	2.7	3.4	2.0	0	8.6	8.9	106

Note: Decrease in conversions and selectivity to others after addition of PPh_3 considered to be from dilution of products to below the GC detection limits and possible degradation.

[a] 10.0 g decane, 50 mg AIBN.

[b] 7.69 g decane, 30 mg AIBN.

[c] C_{10}-one = decanone, C_{10}-ol = decanol and acid = carboxylic acid.

Table 4
Oxidation of *n*-decane using AIBN with and without catalyst.[a]

Initiator/catalyst	Conversion%	Selectivity%					
		C_{10} ketones	C_{10} internal alcohols	C_{10} terminal alcohols	C_{10} diones	C_1–C_9 acids	Others
Blank	0.028	55.3	13.2	0	0	0	31.5
AIBN	1.13	64.4	7.5	1.9	12.3	7.0	6.9
$NanoCeO_2$	0.11	27.7	17.7	4.4	11.3	24.6	14.3
AIBN + $nanoCeO_2$	0.78	24.3	25.3	1.4	11.0	22.0	16.0
AIBN + Aldrich CeO_2	1.13	45.5	17.4	1.7	15.3	10.6	9.5
AIBN + TiO_2	0.58	34.6	29.8	1.9	5.4	10.3	18.0
AIBN + ZSM-5	0.91	56.8	12.5	2.4	10.8	8.6	8.9

[a] Decane (7.69 g), AIBN (30 mg), catalyst (100 mg), 20 h, 90 °C, 1.2 MPa O_2.

Table 5
Epoxidation of 1-octene with catalyst and initiator.[a]

Initiator/catalyst	Conversion%	1,2-Epoxyoctane selectivity%
AIBN	8.5	12
AIBN + $Au/nanoCeO_2$	14.6	10
AIBN + $nanoCeO_2$	9.2	13

[a] 1-Octene (6.06 g), catalyst (100 mg) initiator (30 mg), 2 h, 90 °C, 1.2 MPa O_2.

alcohols:ketones ratio was increased, although not as much as using $nanoCeO_2$ and AIBN. Addition of TiO_2 with AIBN was found to have a lower conversion for the oxidation of decane than AIBN alone, and the alcohols:ketones ratio was higher than using AIBN alone but not as high as over $nanoCeO_2$ and AIBN. ZSM-5 with AIBN was found to give only a slightly lower conversion than AIBN alone for the oxidation of decane, and the alcohols:ketones ratio was also only slightly higher than over AIBN alone. The results imply that the accessible surface area of the catalyst exerts an influence on the product distribution, but that the exact nature of the surface sites may not be critical. The decrease in conversion over $Au/nanoCeO_2$, $nanoCeO_2$ and TiO_2 indicates that these materials are interacting with the radicals formed. The change in the product distribution observed suggests that this is selective for peroxy radicals which are decomposed selectively to alcohols. Corma and co-workers have previously described radical trapping with Au [12,13] but the results from this study suggest that Au is not needed.

The $Au/nanoCeO_2$ catalyst was also tested for the less demanding epoxidation of 1-octene, one of the reactions for which Corma and co-workers [12] reported the catalyst to be active in the presence of AIBN. Similarly, our catalyst was found to have low activity until AIBN was added (Table 5). The conversion observed over the $Au/nanoCeO_2$ with AIBN present was significantly higher than the blank AIBN reaction, as previously reported [12]. The detected conversion (14.6%) was, however, higher and the epoxide selectivity (10.4%) lower than reported by Corma and co-workers under similar conditions (conversion ≈ 4%, selectivity ≈ 50%). These variations may be caused by differences in the catalyst preparation procedure, precursor materials and testing conditions being used. The $nanoCeO_2$ support was also tested for the epoxidation of 1-octene and was found in combination with AIBN, not to significantly change the conversion compared to AIBN alone (Table 5). This lack of selectivity could indicate that the AIBN-Au compounds formed in Corma's study are not replicated here.

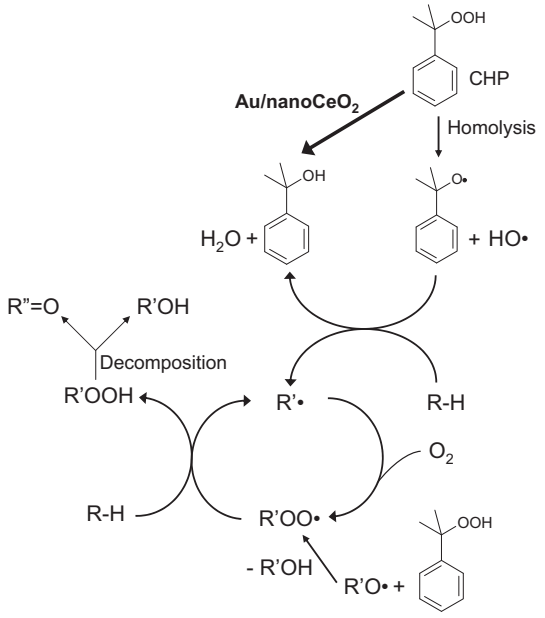

Fig. 5. Proposed reaction scheme for the oxidation of decane (R–H) with CHP. R′ = $C_{10}H_{21}$ or $PhC(Me)_2$, R″ = $C_{10}H_{20}$. Reduction of CHP by $Au/nanoCeO_2$ also shown in bold (thick arrow). Consecutive reactions to form diones and acids excluded from scheme for simplicity.

Decane oxidation was also performed using the radical initiator CHP with and without the $Au/nanoCeO_2$ catalyst (Table 6). CHP was found to be active for the oxidation of decane but not as active as AIBN. The higher activity of AIBN is attributed to its greater efficiency in producing radicals. AIBN produces more radicals for a variety of reasons including: it more readily decomposes generating more radical species under the same conditions [34], and it is an azo-compound that only decomposes homolytically giving two C-centred radicals, while CHP can be decomposed by traces of acids (to give no radicals) and by radical induced decomposition (one radical gives rise to one radical) as well as by homolysis (giving 2 radicals); as shown in Fig. 4.

Table 6
Oxidation of decane using CHP with and without $Au/nanoCeO_2$ catalyst.[a]

Catalyst/initiator	Conversion%	Selectivity%				
		C_{10} ketones	C_{10} internal alcohols	C_{10} terminal alcohols	C_1–C_9 acids	Others
CHP	0.15	24.8	6.1	0.2	2.5	66.4
CHP + $Au/nanoCeO_2$	0.036	76.5	0.5	0	6.5	16.5

[a] Decane (7.69 g), CHP (30 mg), $Au/nanoCeO_2$ catalyst (100 mg), 2 h, 90 °C, 1.2 MPa O_2.

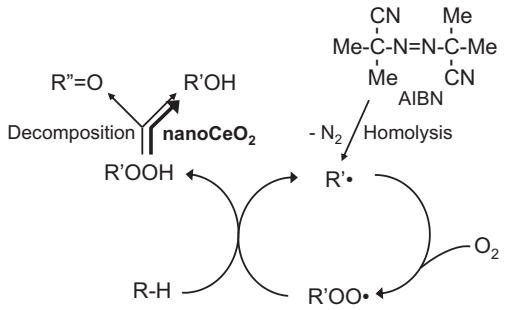

Fig. 6. Proposed reaction scheme for the oxidation of decane (R–H) with AIBN. R′ = $C_{10}H_{21}$ or $Me_2C(CN)$, R″ = $C_{10}H_{20}$. Selective reduction of R′OOH to R′OH on addition of nano ceria based catalysts also shown in bold (thick arrow). Consecutive reactions to form diones and acids excluded from scheme for simplicity.

Addition of Au/nanoCeO_2 with CHP was found to significantly reduce the decane conversion, as compared to the reaction with CHP alone. For both the CHP and Au/nanoCeO_2 with CHP reactions, the radical initiator was found to completely decompose during the reaction. The main decomposition products of CHP from the reaction without Au/nanoCeO_2 were acetophenone (the ketone product) and 2-phenyl-2-propanol (the alcohol product), in approximately a 50:50 ratio. However, for the CHP with Au/nanoCeO_2 reaction, the radical initiator was found to decompose almost entirely into 2-phenyl-2-propanol. The Au/nanoCeO_2 catalyst therefore selectively reduces CHP to the alcohol that is consistent with previously reported findings [10]. This reduction of CHP by Au/nanoCeO_2 may prevent the formation of decane peroxides and thus explain the lower conversion observed (Fig. 5).

The ability of Au/nanoCeO_2 to selectively reduce hydroperoxides to alcohols, as observed in the presence of CHP, may also explain the slight increase in the alcohols:ketones ratio observed for the oxidation of decane with AIBN and Au/nanoCeO_2 as compared to AIBN alone (Table 2 and Fig. 6). However, Au/nanoCeO_2 is clearly more efficient at selectively converting CHP than decane peroxides under the conditions studied.

The radical initiators CHP and AIBN were found to be active for the oxidation of decane, producing a range of oxygenated products. AIBN was found to be more active under the conditions studied. At higher temperature and pressure, in the presence of AIBN, a higher conversion but lower apparent peroxide selectivities are observed; more peroxides are thus proposed to have been produced but they are considered to have shorter lifetimes. The change in ketone and alcohol selectivities with AIBN under different conditions and compared to using CHP may arise from the different decyl, α-cyanoisopropyl and cumene peroxy radical pathways (shown in Figs. 5 and 6) or from the various isomeric decyl or decylperoxy radical pathways.

4. Conclusions

The combination of AIBN and Au/nanoCeO_2 was found to be active for the oxidation of 1-octene as previously reported [12]. However, the combination of AIBN and Au/nanoCeO_2 does not enhance the conversion in the more challenging oxidation of *n*-decane compared to AIBN alone. Therefore, either radicals from AIBN do not complex to the ceria-based catalysts in the alkane medium or the resulting complex is not active for the oxidation of the alkane. The oxidation of decane in AIBN with either Au/nanoCeO_2 or nanoCeO_2 does, however, slightly increase the alcohol selectivity. Some of the peroxides produced by AIBN are thus considered to be selectively reduced to alcohols over the nanoCeO_2 catalysts.

The highly demanding direct oxidation of decane has been shown to be possible using radical initiators, resulting in the formation of range of oxygenated products. Ceria-based catalysts have been found to be beneficial for the selective functionalisation of hydrocarbons in specific cases. The combination of a gold supported on nano-ceria catalyst and AIBN has been shown to be active for the oxidation of 1-octene, whereas a nano-ceria catalyst and AIBN has been found to modify the selectivity for the oxidation of decane.

Acknowledgments

This work was sponsored by Johnson Matthey and Sasol. Discussion and input from Xavier Baucherel and Mike J. Watson (Johnson Matthey) and Jonathan Chetty and Cathy Dwyer (Sasol) are gratefully acknowledged. Sarwat Iqbal helped with the AAS measurement. Sivaram Pradhan calcined the ZSM-5 catalyst.

References

[1] G. Centi, F. Cavani, F. Trifirò, Selective Oxidation by Heterogeneous Catalysis, Kluwer Academic/Plenum, New York, London, 2001.
[2] I. Hermans, J. Peeters, P. Jacobs, Top. Catal. 48 (2008) 41–48.
[3] Anonymous, Chem. Week 165 (2003) 33.
[4] C.E. Frank, Chem. Rev. 46 (1950) 155–169.
[5] D.M. Brown, A. Fish, Proc. Roy. Soc. Lond. Ser. A 308 (1969) 547–568.
[6] K.U. Ingold, Chem. Rev. 61 (2002) 563–589.
[7] G.H. Twigg, Chem. Eng. Sci. 3 (1954) 5–16.
[8] M.D. Hughes, Y.-J. Xu, P. Jenkins, P. McMorn, P. Landon, D.I. Enache, A.F. Carley, G.A. Attard, G.J. Hutchings, F. King, E.H. Stitt, P. Johnston, K. Griffin, C.J. Kiely, Nature 437 (2005) 1132–1135.
[9] J. Schwank, Gold Bull. 16 (1983) 103–110.
[10] T. Uchida, M. Wakakura, A. Miyake, T. Ogawa, J. Therm. Anal. Calorim. 93 (2008) 47–52.
[11] M. Álvaro, C. Aprile, A. Corma, B. Ferrer, H. García, J. Catal. 245 (2007) 249–252.
[12] C. Aprile, A. Corma, M.E. Domine, H. Garcia, C. Mitchell, J. Catal. 264 (2009) 44–53.
[13] C. Aprile, M. Boronat, B. Ferrer, A. Corma, H. Garcia, J. Am. Chem. Soc. 128 (2006) 8388–8389.
[14] A. Goosen, C.W. McCleland, D.H. Morgan, J.S. O'Connell, A. Ramplin, J. Chem. Soc., Perkin Trans. 1 (1993) 401–402.
[15] G.S. Hammond, C.-H.S. Wu, O.D. Trapp, J. Warkentin, R.T. Keys, J. Am. Chem. Soc. 82 (1960) 5394–5399.
[16] C.-H.S. Wu, G.S. Hammond, J.M. Wright, J. Am. Chem. Soc. 82 (1960) 5386–5394.
[17] G.S. Hammond, O.D. Trapp, R.T. Keys, D.L. Neff, J. Am. Chem. Soc. 81 (1959) 4878–4882.
[18] C. Walling, J. Polym. Sci. 14 (1954) 214–217.
[19] L.-X. Xu, C.-H. He, M.-Q. Zhu, K.-J. Wu, Y.-L. Lai, Catal. Lett. 118 (2007) 248–253.
[20] G. Lü, D. Ji, G. Qian, Y. Qi, X. Wang, J. Suo, Appl. Catal., A 280 (2005) 175–180.
[21] G. Lü, R. Zhao, G. Qian, Y. Qi, X. Wang, J. Suo, Catal. Lett. 97 (2004) 115–118.
[22] Y.-J. Xu, P. Landon, D. Enache, A.F. Carley, M.W. Roberts, G.J. Hutchings, Catal. Lett. 101 (2005) 175–179.
[23] L.-X. Xu, C.-H. He, M.-Q. Zhu, S. Fang, Catal. Lett. 114 (2007) 202–205.
[24] R. Zhao, D. Ji, G. Lv, G. Qian, L. Yan, X. Wang, J. Suo, Chem. Commun. (2004) 904–905.
[25] K. Zhu, J. Hu, R. Richards, Catal. Lett. 100 (2005) 195–199.
[26] L. Chen, J. Hu, R. Richards, J. Am. Chem. Soc. 131 (2008) 914–915.
[27] B.P.C. Hereijgers, B.M. Weckhuysen, J. Catal. 270 (2010) 16–25.
[28] E.D. Mark, J. Chem. Technol. Biotechnol. 77 (2002) 43–50.
[29] J. Knaut, H.J. Richtler, J. Am. Oil Chem. Soc. 62 (1985) 317–327.
[30] C.F. Cullis, M.M. Hirschler, R.L. Rogers, Proc. Roy. Soc. Lond. Ser. A 375 (1981) 543–563.
[31] B. Zhan, B. Modén, J. Dakka, J.G. Santiesteban, E. Iglesia, J. Catal. 245 (2007) 316–325.
[32] G.B. Shul'pin, J. Mol. Catal. A: Chem. 189 (2002) 39–66.
[33] G.B. Shul'pin, D. Attanasio, L. Suber, J. Catal. 142 (1993) 147–152.
[34] J. Meijer, A. Hogt, Acros Org. Rev. (2006) 1–11.
[35] K. Weissermel, H.-J. Arpe, Industrial Organic Chemistry, WILEY-VCH, Weinheim, 2003. ch. 7, pp. 174-176.